Earthquake Engineering, Tenth World Conference © 1992 Balkema, Rotterdam. ISBN 90 5410 060 5

Study on restoring force characteristics of X-steel braces

Takahashi Yasuhiko
Obayashi Technical Research Institute, Tokyo, Japan

Nakamura Noriyoshi
The Tokyo Electric Power Company Inc., Japan

Kato Ben
Toyo University, Tokyo, Japan

Saeki Toshio
Kajima Technical Research Institute, Tokyo, Japan

ABSTRACT : A large scale model test of X-type steel braces, which are important seismic elements in steel frames of nuclear power station buildings, was conducted within the parameters of joint type, slenderness ratio and width-to-thickness ratio. A lot of test results, on strength, deformation characteristics and failure modes, were examined, on the basis of generalized effective slenderness ratio of brace in order to set up a model of restoring force characteristics.

This continues to the following two papers: 「Model of restoring force characteristics of X-steel braces(in Topic No.9)」 and 「Nonlinear dynamic analysis of X-steel braces for design use(in Topic No.9 or 10)」,pronounced in 10th WCEE. The main object of this series is to propose simplified and reasonable restoring force characteristics available for the dynamic nonlinear seismic response analysis of general X-braced buildings.

1 INTRODUCTION

In seismic countries as well as in Japan, it is effective to perform dynamic nonlinear seismic response analysis, using reasonable restoring force characteristics in order to design structures,estimating quantitatively their seismic safety during large scale earthquakes.

Steel structures in nuclear power station buildings are usually designed so that resistance to earthquake laod is taken up in the X-type braces. Consequently, it is necessary to investigate and formulate the elasto-plastic behavior of X-braces.

However, currently there is very little knowlegde concerning the behavior of X-braces, not only in nuclear power station buildings but also in general buildings, to evaluate the restoring force characteristics of the steel frames.

The authors conducted a large scale model test of X-braces and in the process collected many test results that were necessary to set up a model of restoring force characteristics.

2 OUTLINE OF THE EXPERIMENT

2.1 Features of steel structure in nuclear power station buildings

The principal factors influencing the restoring force characteristics of braces are thought to be,the slenderness ratio, the width-to-thickness ratio of braces,and the restraining effect of braces due to a difference of joint types. Therefore, investigations of the actual braced frames in view of these factors were made.

Table 1 shows the dimensions of X-braced frames and the structural properties of brace members(H-shape member), indicated with an SS41 equivalent. Fig.1 shows three types of joints in braces: a bracket type (henceforth: B Type), a composite gusset plate type(C Type) and a double gusset plate type(D Type).

2.2 Specimens

Experiments were conducted within three parameters of slenderness ratio (λ =40,60 ,80, $\lambda = L/i_y$, where L: half the length of the X-brace, Table 1 ,and where i_y: the radius of gyration of the area on the weak axis),the flange width-to-thickness ratio (B/t_f=6,9,13, where B: half the width of the flange,and where t_f: flange thickness) and joint types(B,C,D-type, Fig.1)existing at both ends of the brace, in reference to Table 1 to investigate the elasto-plastic hysteretic characteristics of X-braces. Experiments were performed on nine reduced scale (1/2.5 or 1/3.5) models simulating standard frame dimensions and details. The combination of the parameters and the

meaning of the specimen names is shown in Table 2 . Specimens were large scale one bay-one storied frames. Three typical configurations of specimens are shown in Fig.2. The height and span of the standard specimens was three meters, and nearly equivalent to the dimensions of actual general buildings.

H-shape members from H-155*155*6*12 to H-110*110*6*6 were used as X-braces according to λ and B/t_f. The joints were arranged at the same place as in the actual structures, using high strength, friction type bolted connections and designed to be stronger than the yield strength of the braces. However both columns and beam were less rigid than usual, because the object of this experiment was to investigate the behavior of the braces themselves.

SS41 was the material used for the braces and the material properties are shown in Table 3 .

Table 3 Material properties

Test piece	Upper yield point σ_y (tonf/cm²)	Tensile strength σ_u (tonf/cm²)	$\frac{\sigma_y}{\sigma_u}$	Rupture strain (%)
ℓ-6	3.77	4.98	0.757	22.4
ℓ-9	2.88	4.41	0.654	29.0
ℓ-12	2.70	4.32	0.626	31.2

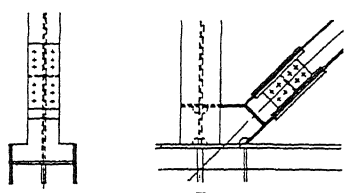

Bracket Type
(B -Type)

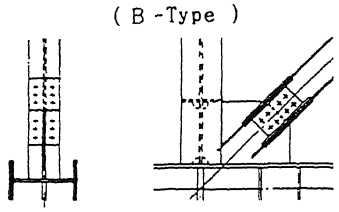

Composite Gusset Plate Type
(C-Type)

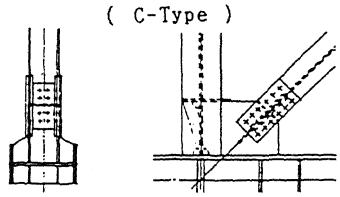

Double Gusset Plate Type
(D-Type)

Fig. 1 Three joint types

Table 1 Tendencies of X-braced frames

			X Braced Frame		
Rigid Frame	Dimensions		Average S : H = 1 : 1 S = H = 7.0m L = 5.0m	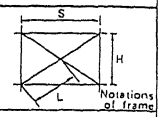	
	Steel Variety		SM50 (PWR type) SS41 (BWR type)		
Brace			Minimum	Mean	Maximum
	Slenderness ratio		35	60	90
	Width-to-thickness ratio	Flange	4	8.5	14.5
		Web	12	25	40

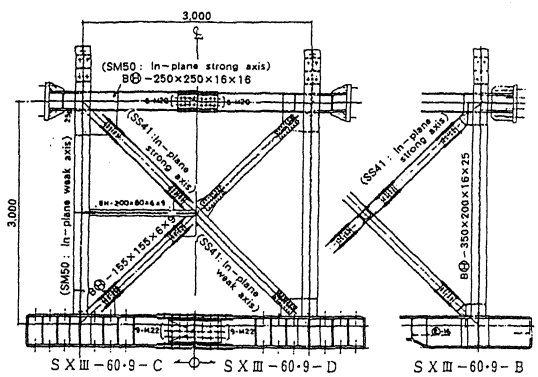

Fig. 2 Configuration of spesimens

Table 2 List of specimens

Brace Member			Joint Type			Dimensions of Rigid Frame
λ	$\frac{b}{t_f}$	Section Size	Bracket Type (B Type)	Composite Gusset Plate Type (C Type)	Double Gusset Plate Type (D Type)	
40	6.0	H-155×155×6×12 (35*1, 6.5*2)	SX II-40·6-B *3	—	—	S=H= 2.0m
	9.0	H-155×155×6×9 (36, 8.6)	SX II-40·9-B	—	—	
60	6.0	H-155×155×6×12 (52, 6.5)	SX III-60·6-B	—	—	S=H= 3.0m
	9.0	H-155×155×6×9 (55, 8.6)	SX III-60·9-B	SX III-60·9-C	SX III-60·9-D	
	13.0	H-155×155×6×6 (57, 12.9)	SX III-60·13-B	—	—	
80	9.0	H-110×110×6×6 (80, 9.4)	SX III-80·9-B	SX III-80·6-C	—	
Remarks			Rigid Frame Specimen SO II : S=H=2.00m SO III : S=H=3.00m			

*1 : Actual slenderness ratio

*2 : Actual width-to-thickness ratio

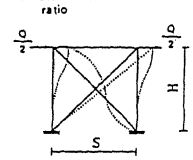

*3 : Meaning of Specimen Name

Ex.) S X II-40·6-B

- Joint type
- Flange width-to-thickness ratio of brace (b/tf)
- Slenderness ratio of brace (λ)
- Dimensions of rigid frame
  - III : 3.0m (height of story and span)
  - II : 2.0m (height of story and span)
- Existence of brace
  - X : Specimen with X type brace
  - O : Specimen without brace
- S signifies steel construction

2.3 Loading method

The foundation beam of the specimen was fixed to the test bed, and the lateral load equivalent to an earthquake was applied to both the left and the right ends of the beam by two actuators, under conditions of no axial force to the columns. The test was done beyond the buckling and the yielding point of the braces under incremental repeated load, whose pattern is shown in Fig. 3.

3 CONSIDERATION OF THE TEST RESULTS

The hysteretic relationships between the shearing force (q) shared by the braces themselves and the shearing deformation angle (γ), and the relationships of the envelop curves of $q - \gamma$ are shown in Fig. 4 and Fig. 5 respectively. q is the shearing force normalized by the yielding axial force of the braces and γ is the shearing deformation angle normalized by the heigth of the specimen.

The initial rigidity of the 6 specimens except SXII-40·6-B, SX II-40·9-B and SXIII-60·9-D, gradually decreased because of the occurrence of flexal buckling and the

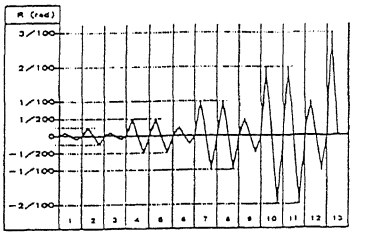

Fig. 3 Loading pattern

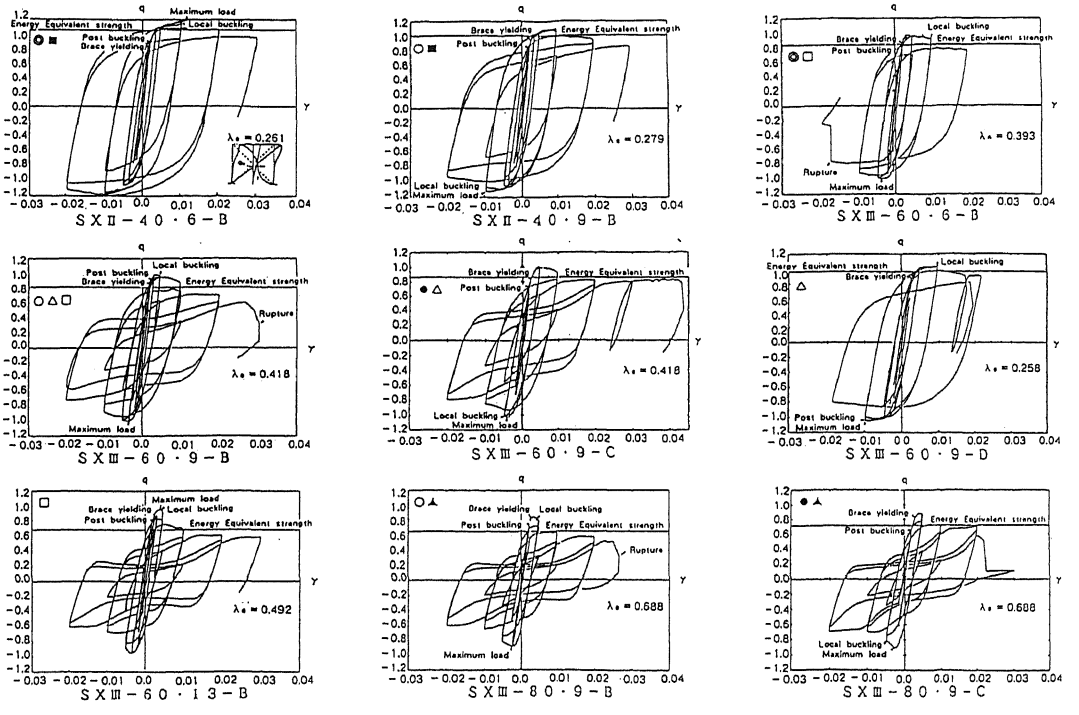

Fig. 4 Normalized load-deformation relationships ($q - \gamma$ curves)

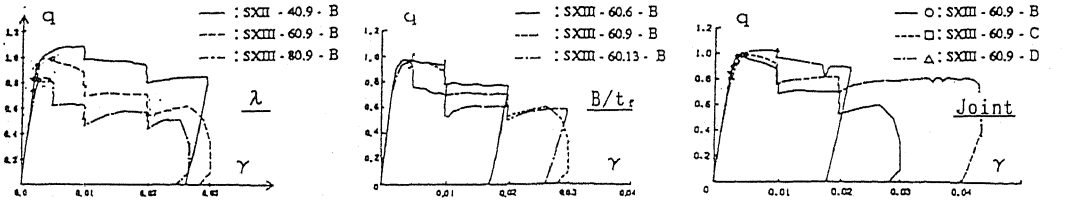

Fig. 5 Envelop curves of $q - \gamma$ relationships

subsequent yielding of the braces. The $q-\gamma$ curves had a negative slope after the attainment of maximum load-carrying capacity. Then local buckling of flanges was observed both at the center and at the ends of the braces, resulting finally in failure.

However in three specimens having stubby braces : SXII-40·6-B, SX II-40·9-B and SX III-60·9-D, yielding occurred before flexal buckling and local buckling took place earlier than the attainment of maximum load. They had very stable hysteretic characteristics before γ reached 1/100. Observing Fig.4 and Fig.5, the $q-\gamma$ relationships of the former have a degrading bi or tri-linear skelton curve and hysteretic characteristics, combined with elasto-plastic type and pinching type. The $q-\gamma$ curves of the latter show bi-linear skelton and stable spindle type hysteresis loops.

The change of buckling mode due to a reversal of the loading direction caused a rapid increase of deformation and S-shape loops.

Flexal buckling modes are shown in Fig. 6. Braces with B joint had an out-of-plane buckling mode. The ends of these braces are assumed to be a pinned and fixed support in structural design. Braces with C joint had an out-of-plane mode and the constraining effect of joint is considered to be similar to ones with B type. Braces with D joint had an in-plane buckling mode. Both ends of these braces are considered to be fixed in design.

Local buckling of the flange played an important role in deformation and the degradation of load carrying capacities. The larger B/t_f was, the earlier local buckling occurred, resulting in a larger deterioration of strength.

The photographs in Fig.7 show some typical failure modes of braces. Photo. (a) shows breakage at the parts with local buckling, which was observed in specimens whose λ were 80. Breakage at the welded part of the crossing joint in X-braces is shown in Photo. (b). Stress concentration and material hardening in the zone affected by the heat from welding caused brittle fracture. Photo. (c) shows breackage at connecting portions, that have a reduced sectional area. It is guessed that secondary bending moments due to both deflection and axial force in the brace caused the unexpected failure. Failure of all specimens occurred when γ was above 2/100 and they showed good deformation capacities.

To examine the deformation capacity, the average accumulative inelastic deformation ratio : η (Eq. (1)), which is the ratio of accumulative inelastic strain energy ΣW to the elastic limit strain energy W_e, is introduced.

$$\eta = \Sigma W / 4 W_e \qquad \text{Eq. (1)}$$

The relationships between η, calculated from the $q-\gamma$ curves of braces, and the cycle of loading are shown in Fig.8. η gradually increases in accordance with the spread of the amplitude of deformation with load reversal. However η is under the influence of not only λ and B/t_f, but also ultimate deformation and failure mode.

Joint type	Bracket type	Composite gusset plate type	Double gusset plate type
Buckling direction	Out-of-plane	Out-of-plane	In-plane
Buckling mode	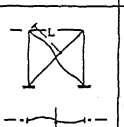	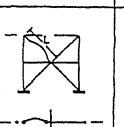	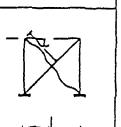
Effective length	0.65L	0.65L	0.40L

Fig. 6 Buckling mode

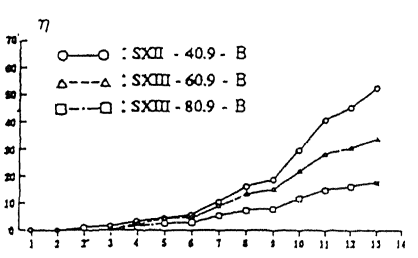

Fig. 8 Accumulative inelastic strain deformation ratio

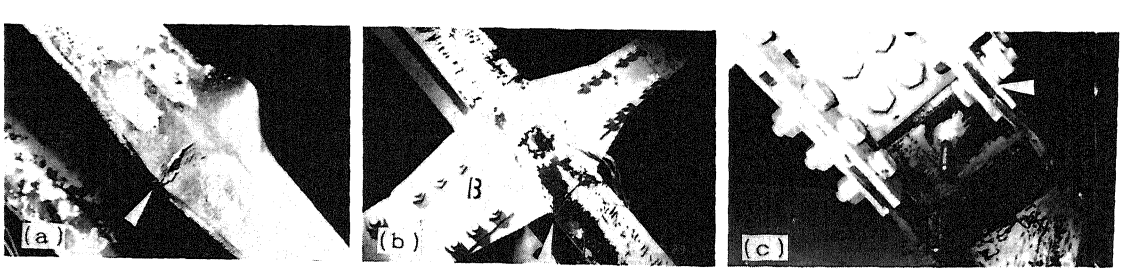

Fig. 7 Failure mode

4 DISCUSSIONS

4.1 Influence of three parameters

The influence of 3 parameters: λ, B/t_f and joint type, on $q-\gamma$ curves and capacity of energy absorption is investigated.

・Slenderness Ratio(λ)

Comparing the test results from three specimens: SXII-40・9-B, SX III-60・9-B and SXIII - 80・9-B, the difference of behavior caused by a variety of λ :40,60,80, can be grasped under the common conditions, that B/t_f is 9 and B joint is adopted. Specimens having a small λ have greater strength and capacity of energy absorption than specimens with a large λ. The hysteretic loop of the former is a stable spindle shape. However the behavior of the latter is S-shape and the deterioration of its load carrying capacity is eminent.

・Width to Thickness Ratio (B/t_f)

Comparing SXIII-60・6-B, SXIII-60・9-B and SXIII -60・13-B, the difference of behavior by varying B/t_f (6,9,13) under the same conditions (λ=60, B type), is investigated. The larger B/t_f is, the less the deformation is, at which local buckling occurs and the clearer the tendency of the degradation of load carrying capacity is.

In addition, it seems that specimen with λ = 60 and B/t_f=6 has almost the same behavior as one with λ = 40 and B/t_f=9.

・Joint Type

The difference in behavior by joint type can be examined, comparing SXIII-60・9-B, SXIII-60・9-C and SXIII-60・9-D. Specimen with B joint has the same hysteretic characteristics as one with C type and the behavior of specimen having D type is more stable and better. However because of failure occurred at the welded section when γ reached 2/100, η is smaller than in the others.

In addition, it seems that specimen with λ = 60 and D type has almost the same behavior as one with λ = 40 and B type.

4.2 Effective buckling length and strength

The joints affect the $q-\gamma$ relationship because joints, composed of gusset plates and splice plates, constraint deformation and rotation. The restraining effect of joints can be evaluated in terms of the effective buckling length: αL (where α is the coefficient of buckling length). Firstly the deformation mode of the brace after buckling is exactly examined to determine the value of α and the following coefficients are adopted.

α =0.65 ;Bracket type and Composite gusset plate type

α =0.40 ;Double gusset plate type

Substituting these α and the material properties into Eq.(2), the generalized slenderness ratio (λ_e) is caluculated.

$$\lambda_e = \alpha \cdot \frac{L}{i_y} \cdot \sqrt{\frac{\sigma_y}{E\pi^2}} \qquad \text{Eq. (2)}$$

where E : Young's modulus

σ_y : Yield strength

λ_e of specimens is described in Fig. 4.

Next in order to evaluate λ_e : that is, the α values, the maximum strength of the X-brace obtained with the test is compared to the theoretical strength calculated by the superposition of the buckling strength and the yielding tensil force. The buckling strength is calculated with a column curve of the A.I.J standard.

Fig.9 shows that the test results are in good agreement with the calculated value. Therefore it is clarified that the restraining effect of both joints are quite high and that the value of the coefficient of α for the buckling length mentioned above is reasonable enough to use in structural design.

Consequently it is possible to analysis the behavior of braces on the basis of only λ_e and B/t_f .

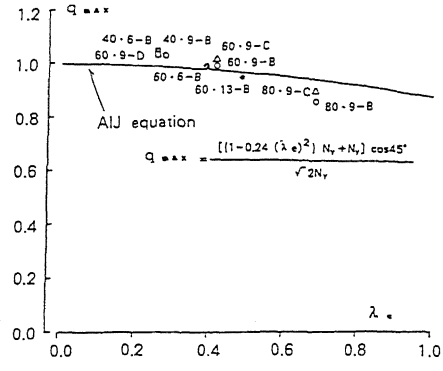

Fig. 9 Relation of maximum strength and slenderness ratio

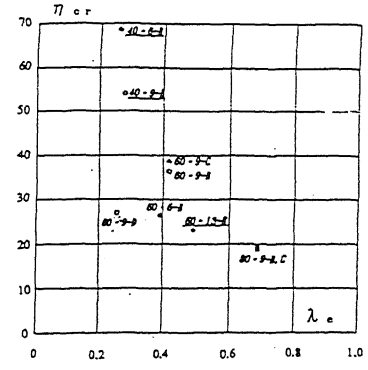

Fig. 10
Deformation capacity of X-braces

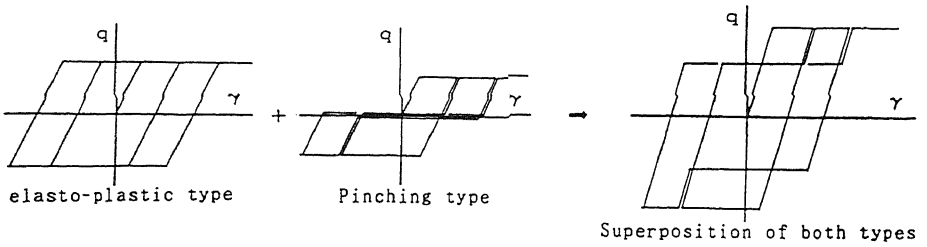

Fig. 11 Image of restoring force characteristic

4.3 Energy absorption

η_{cr} is defined as the average accumulative inelastic deformation ratio (η) at the ultimate state and the relationships between η_{cr} and λ_e is shown in Fig.10. It is evident that the larger λ_e is, the smaller η_{cr} is and η_{cr} is greater than 20. However it seems that the correlation between η_{cr} and B/t_f is not clear. It is possible to use η_{cr} as the lower limit value of deformation capacity.

4.4 Characteristic shape of the restoring force

The $q-\gamma$ relationship has a degrading bi linear or tri-linear skelton curve. The hysteretic characteristics depend upon λ_e and B/t_f: where λ_e is small, the characteristics show a stable spindle shape, but where λ_e is large, they show a combination of the perfect elasto-plastic and the pinching type shape. The hysteretic characteristics of the specimen having a larger λ_e tend to show that pinching occuers at smaller deformations and at lower loads. Also the higher B/t_f is, the earlier local buckling occurs and the larger the strength deterioration.

If the skelton curve of X-brace can be expressed as a simple bi-linear relationship, the restoring force characteristic will be a model in combination with the perfect elasto-plastic type and the pinching type, on the basis of the slenderness ratio and the width-to-thickness ratio, shown in Fig.11.

5 CONCLUDING REMARKS

A large scale model test of X-brace which is the principal earthquake resistant element of steel buildings, was conducted to obtain a lot of useful information to set up simple and reasonable restoring force characteristics.

The load-deformation relationships have a degrading bi or tri-linear skelton curve and the hysteretic characteristics show the behavior with a combination of the perfect elasto-plastic type and the pinching type shapes. This elasto-plastic behavior and the strength of X-braces depends upon the effective slenderness ratio, considering the restraining effect of both end joints, and the width-to-thickness ratio of flange. The deformation capacity can be evaluated with the accumulative inelastic deformation ratio which is greatly influenced by the failure mode of braces.

ACKNOWLEDGEMENTS

This study was carried out, as a part of joint reseach study on restoring force characteristics of the steel frames of nuclear power station buildings, by ten Japanese electric power companieis (Tokyo, Hokkaido, Tohoku, Chubu, Hokuriku, Kansai, Chugoku, Shikoku, Kyushu and Japan Atomic) in cooperation with five construction companies (Obayashi, Kajima, Shimizu, Taisei, Takenaka). The work was performed under the guidance of reseach committee, chaired by Professor Emeritus Ben Kato of the University of Tokyo. The authers wish to acknowledge the valuable cooperation and suggestions provided by the members of the committee.

REFERENCES

Architectural Institute of Japan. Design Standard for Steel Structures. 1973

Kato B., Nakamura N. et al. 1990. Study on Restoring Force Characteristics of Steel Frames in Buildings of Nuclear Power Station (Part 1～10), Technical Papers of Annual Meeting, A.I.J: 1531-1544

Kato B. and Akiyama H.. 1977. Restoring Force Characteristics of Steel Frames Equipped with Diagonal Bracings, Trans. A.I.J: 99-107